

Electric fields are novel determinants of human macrophage functions

Joseph I. Hoare, Ann M. Rajnicek, Colin D. McCaig, Robert N. Barker,
and Heather M. Wilson¹

School of Medicine, Medical Sciences and Nutrition, University of Aberdeen, Institute of Medical Sciences, Foresterhill, Aberdeen,
United Kingdom

RECEIVED AUGUST 31, 2015; REVISED DECEMBER 2, 2015; ACCEPTED DECEMBER 18, 2015. DOI: 10.1189/jlb.3A0815-390R

ABSTRACT

Macrophages are key cells in inflammation and repair, and their activity requires close regulation. The characterization of cues coordinating macrophage function has focused on biologic and soluble mediators, with little known about their responses to physical stimuli, such as the electrical fields that are generated naturally in injured tissue and which accelerate wound healing. To address this gap in understanding, we tested how properties of human monocyte-derived macrophages are regulated by applied electrical fields, similar in strengths to those established naturally. With the use of live-cell video microscopy, we show that macrophage migration is directed anodally by electrical fields as low as 5 mV/mm and is electrical field strength dependent, with effects peaking ~300 mV/mm. Monocytes, as macrophage precursors, migrate in the opposite, cathodal direction. Strikingly, we show for the first time that electrical fields significantly enhance macrophage phagocytic uptake of a variety of targets, including carboxylate beads, apoptotic neutrophils, and the nominal opportunist pathogen *Candida albicans*, which engage different classes of surface receptors. These electrical field-induced functional changes are accompanied by clustering of phagocytic receptors, enhanced PI3K and ERK activation, mobilization of intracellular calcium, and actin polarization. Electrical fields also modulate cytokine production selectively and can augment some effects of conventional polarizing stimuli on cytokine secretion. Taken together, electrical signals have been identified as major contributors to the coordination and regulation of important human macrophage functions, including those essential for microbial clearance and healing. Our results open up a new area of research into effects of naturally occurring and clinically applied electrical fields in conditions where macrophage activity is critical. *J. Leukoc. Biol.* 99: 1141–1151; 2016.

Abbreviations: AM = acetoxymethyl ester, Ca²⁺ = calcium, CTCF = cell total corrected fluorescence, EF = electric(al) field, M1 = classically activated macrophage, M2 = alternatively activated macrophage, NT3 = neurotrophin-3, p = phosphorylated, PI = phagocytic index, T = time (hours), Td = displacement, Td/T = velocity of cell displacement, Tt = total migration distance, Tt/T = migration velocity, VEGF = vascular endothelial growth factor

The online version of this paper, found at www.jleukbio.org, includes supplemental information.

Introduction

Macrophages are heterogeneous cells that play key roles in host defense and tissue repair following challenges from injury, infection, or malignancy [1, 2]. The ability to coordinate many specialized effector functions equips macrophages for these roles, and their dysregulation contributes to chronic inflammatory disease, autoimmunity, tumorigenesis, or fibrosis. Macrophage functions are determined by the integration of signals from the microenvironment that to date, have been predominantly characterized as biologic and chemical stimuli, such as microbial products, cytokines, and metabolic factors. Bacterial LPS and IFN- γ (M1 activation), for example, can drive the proinflammatory, tissue-destructive properties of macrophages, whereas IL-4 (M2 activation) induces polarization to a more tissue-reparative phenotype [1]. These biochemical factors also influence phagocytic and chemokine receptor expression and migratory responses of macrophages. Recent findings, however, have begun to challenge this paradigm, raising the prospect that physical factors, present in a complex microenvironment, also regulate macrophage activity. These suggestions arise from demonstrations that for example, substrate topography, cell elongation, and elasticity influence polarization of macrophage phenotype [3–5] and that externally applied ultrasound or electromagnetic fields affect macrophage responses to bacterial challenge [6, 7]. One potentially important physical cue that has been overlooked in the regulation of macrophage functions is the endogenous, direct current EF.

Situations where EFs arise include wounded tissues, where epithelial barriers have been broken. For example, directional ion transport leads to a *trans*-epithelial potential difference of 50–100 mV across intact skin. This collapses locally to 0 at the breached epithelium, giving rise to a steady voltage gradient of 40–200 mV/mm directed toward the wound edge and parallel to the epithelial layer, with the wound negative with respect to distal tissue [8–10]. Endogenous EFs accelerate the wound-healing process, an effect attributed to the strong directional guidance cues for the migration of fibroblasts and keratinocytes [11, 12].

1. Correspondence: School of Medicine, Medical Sciences and Nutrition, University of Aberdeen, Institute of Medical Sciences, Foresterhill, Aberdeen, AB25 2ZD, UK. E-mail: h.m.wilson@abdn.ac.uk

However, the effects of direct current EFs on human macrophages remain to be established, although these cells are prominent in inflamed or injured tissue, and their loss is detrimental to wound resolution [1, 2, 13, 14]. Macrophages facilitate healing by a number of mechanisms, including promotion and resolution of inflammation and phagocytosis of cell debris, apoptotic cells, and microbes. They also secrete a variety of factors, including cytokines, providing support for angiogenesis, extracellular matrix synthesis, fibroblast proliferation, and epithelialization, thereby facilitating regeneration of the injured tissue.

Given the importance of regulating macrophage activity in situations where EFs occur, we sought to determine if human macrophages do respond to EF signals, in particular, by changing their migration pattern or functional properties. We report that human monocyte-derived macrophages react to physiologic strength EFs with strong polarized and directed migration toward the anode and exhibit significantly enhanced phagocytic uptake and cytokine secretion. Molecular mechanisms that may underlie these EF-induced effects are also identified. By establishing that EFs are a potent physical stimulus regulating multiple macrophage activities, this work introduces the exciting new concept that wound-induced or clinically applied EFs may act as potent coordinators of macrophage responses, for example, during tissue repair.

MATERIALS AND METHODS

Cell isolation

Human monocyte-derived macrophages and neutrophils were isolated from blood of healthy adult-consenting donors, as approved by the Ethics Review Board of the College of Life Sciences and Medicine, University of Aberdeen. Neutrophils and PBMCs were fractionated by density gradient centrifugation. Monocytes were isolated from the PBMCs by positive selection using human CD14 microbeads to ensure a highly purified population (Miltenyi Biotec, Bergisch Gladbach, Germany) and differentiated into macrophages over 7 d in DMEM (Lonza, Basel, Switzerland), supplemented with 1% L-glutamine, 2% penicillin/streptomycin, and 10% human AB⁺ serum [15]. In selected experiments, M1 and M2 macrophage polarization was, respectively, induced by incubation with IFN- γ (20 ng/ml)/LPS (100 ng/ml) or IL-4 (20 ng/ml) for 24 h.

EF application

Custom-designed chambers for application of EFs were prepared based on a modified version of that described previously [16, 17]. In brief, glass coverslips were used to create a $50 \times 10 \times 0.2$ mm channel within a 9 cm tissue-culture dish. Discrete medium reservoirs were formed at both ends of the channel using silicone grease. Silver/silver chloride electrodes were inserted into Steinberg's buffer reservoirs and connected to the chambers through 2% agar salt bridges. The EF was determined by measuring the voltage across the 50 mm channel with a voltmeter and adjusted using variable resistors. Macrophages were seeded into the central channel and allowed to adhere for 2 h before the application of EFs. EF exposure did not affect cell viability [as assessed by metabolic activity (XTT assay; Life Technologies, Thermo Fisher Scientific, Grand Island, NY, USA) or membrane permeability (Trypan blue exclusion)], which remained $\sim 100\%$ in all experiments. In selected experiments requiring high-resolution imaging, $\sim 0.4 \times 10^6$ macrophages were seeded in μ -Slide i ibiTreat flow chambers (80106; ibidi, Planegg, Germany) and incubated for 2 h for cells to adhere. The ibidi slides are of a similar design as the custom EF chambers (channel dimensions, $50 \times 5 \times 0.4$ mm), and the EF was applied as described above.

Electrotaxis assay analysis

Macrophages were exposed to an EF (5–450 mV/mm) for 2 h at 37°C in a temperature-controlled chamber on an inverted microscope stage. Serial

time-lapse images were recorded at multiple points using a Nikon Eclipse TE2000-U microscope and SimplePCI imaging software (Hamamatsu, Sewickley, PA, USA). Cellular migration was tracked using ImageJ software (Manual Tracking and Chemotaxis Tool plugins; NIH, Bethesda, MD, USA). Cell migration was recorded by tracking nuclear Td between frames at 10 min intervals.

Tt represents the total length (μ m) of the trajectory to which the cell has migrated (Supplemental Fig. 1A). Tt/T represents the total distance migrated (μ m) over T. The Td represents the straight-line distance between the position of the cell at the start (T = 0) and the end (T = 2 h) of the migration assay (Supplemental Fig. 1A).

The directedness of cell migration was defined as cosine θ , where θ is the angle defined by the EF vector (horizontal) and the line of Td. The EF was set up with the anode on the right and cathode on the left of the electrotaxis chambers. The cosine θ values lie between -1 and $+1$ and are presented as the mean directedness index of all events. Therefore, a cell moving directly along the field lines toward the anode would have a directedness of -1 , whereas a cell moving directly to the cathode would have a directedness of $+1$; a mean value close to 0 indicates random migration (Supplemental Fig. 1B).

Cell-shape analysis

The changes in cell shape and orientation were measured from confocal images taken following EF stimulation. Macrophages were exposed to 150 mV/mm for 2 h and then fixed with 8% paraformaldehyde. Images were recorded using a scanning laser confocal microscope (LSM710), and the measurements were performed using the ZEN 2012 (blue edition) software package. The cell area was measured by manually tracing regions of interest around the cell body. The long axis was described as the longest available axis across the cell body and the short axis perpendicular to the long axis, bisecting the nucleus. The elongation ratio was expressed as long axis:short axis. The long axis angle, used to describe the orientation of cells, was described as the angle between the long axis and the horizontal plane, indicated by the line between 0 and 180° (Supplemental Fig. 1C).

Phagocytosis assay

Macrophages (0.5×10^6 – 1.0×10^6) were seeded in custom EF chambers, left to adhere for 2 h, and then exposed to 30–150 mV/mm EF for 2 h. In selected experiments, the PI3K inhibitor LY294002 (10 μ M) was added to macrophage cultures, 1 h before applying an EF. Carboxylate microspheres (10 μ m; Polysciences, Warrington, PA, USA) or *C. albicans* strain CA14CIP10 (provided by Professor Neil Gow, Aberdeen Fungal Group, Aberdeen, United Kingdom) were added at a 3:1 ratio (particle:macrophage) to the macrophage cultures immediately after EF stimulation and then incubated for 2 h at 37°C (5% CO₂). At the end of the incubation period, macrophages were washed thoroughly to remove bound particles that were not phagocytosed. Images were captured using an Axio Observer Z1 inverted microscope (Zeiss, Oberkochen, Germany). Neutrophils were incubated for 24 h at 37°C to induce apoptosis and then added at a 5:1 ratio before incubation for 30 min at 37°C (5% CO₂). Macrophages were fixed in 2% glutaraldehyde and stained with 3,3'-diaminobenzidine peroxidase substrate (Vector Laboratories, Burlingame, CA, USA) for 5 min and images captured using an inverted EVOS XL light microscope. Phagocytic uptake was defined as the percentage of macrophages that contained at least 1 fully engulfed bead, apoptotic neutrophil, or *C. albicans* particle. PI was calculated as the mean number of particles engulfed per phagocytosing macrophage, multiplied by percentage of phagocytic cells.

Immunofluorescence imaging and analysis

Macrophages were exposed to EFs of 150 mV/mm for 2 h and then fixed with 8% paraformaldehyde. Polymerized actin was labeled using rhodamine-conjugated phalloidin (Invitrogen, Thermo Fisher Scientific). The mannose and scavenger receptors were, respectively, labeled using antimannose receptor IgG and antimacrophage scavenger receptor 1 (Abcam, Cambridge, MA, USA), in combination with Alexa Fluor 647. Nuclei were labeled using Vectashield + DAPI (Vector Laboratories). Cells were analyzed using a scanning laser confocal microscope (LSM710), and laser intensities and exposure times were kept constant to allow quantitative comparisons across images and samples. Fluorescence videos and images were analyzed using ImageJ

software (NIH). Individual cells or areas were manually traced as regions of interest and measured. CTCF = integrated density of regions of interest – (area of regions of interest \times mean background fluorescence). In selected experiments, macrophages were preincubated with the specific inhibitors of PI3K (LY294002; 10 μ M), ERK1/2 (U0126; 10 μ M), intracellular Ca^{2+} (BAPTA-AM; 10 μ M), and extracellular Ca^{2+} (BAPTA; 300 μ M) for 30 min before EF application and determination of actin polymerization and receptor-clustering analysis. None of these inhibitors nor their vehicle controls significantly affected basal levels of actin polymerization or receptor clustering in non-EF-exposed macrophages.

Western blotting

Macrophages (9×10^5) were seeded in custom EF chambers, left to adhere for 2 h, and then exposed to 150 mV/mm for 2 h. Protein lysates were prepared from macrophages using lysis buffer. A total of 20 μ g protein was separated by SDS-PAGE and transferred to Hybond-P polyvinylidene difluoride membrane (Amersham, GE Healthcare, Little Chalfont, United Kingdom) for Western blot analysis, with specific primary antibodies for Akt and p-Akt ser473, STAT3 and p-STAT3 tyr705, p38 and p-p38 thr180/tyr182, and ERK and p-ERK thr202/tyr204 (Cell Signaling Technology, Danvers, MA, USA) and β -actin (Sigma-Aldrich, St. Louis, MO, USA). Immunolabeled proteins were detected using appropriate HRP-conjugated secondary antibodies, followed by visualization with ECL (GE Healthcare). Bands were normalized to β -actin.

Intracellular Ca^{2+} measurements

Macrophages were loaded with 2.5 μ M Fluo-4 AM ester for 40 min at 37°C. The slides were then washed with indicator-free medium and incubated for a further 30 min to allow de-esterification. An Axio Observer inverted microscope (Zeiss) was used to capture serial time-lapse fluorescence images (1 frame/5 s) using AxioVision software. During acquisition, 150 mV/mm was applied, or 2 μ M Ca^{2+} ionophore (A23187; Sigma-Aldrich) was added. Images were captured using a $\times 40$ oil-immersion objective and differential interference contrast and FITC images recorded. The recordings were started before any stimulation was added to capture background levels. Fluorescence videos were analyzed using ImageJ software (NIH). The images were converted to grayscale, and regions of interest were traced around individual cells. The CTCF values of selected cells were calculated and tracked across individual frames throughout the recording.

Measurement of cytokine concentrations

Macrophages were seeded at a density of 9×10^5 in custom EF chambers and left to adhere for 2 h. Culture medium was replaced and cultures then exposed to an EF of 150 mV/mm for 2 h. LPS (100 ng/ml) and IFN- γ (20 ng/ml) were added to cell cultures, along with EFs, when appropriate. Cytokine concentrations were measured 24 h after stimulation. Concentrations of TNF- α , IL-1 β , IL-6, CCL2, and IL-23 in cell-culture supernatant were determined using ELISA kits (eBioscience, San Diego, CA, USA), and NT3 was measured using an ELISA kit (Abcam), according to the manufacturers' instructions. IL-10 concentration was determined using ELISA matched antibody pairs (BD Biosciences, San Jose, CA, USA).

Statistical analysis

Statistical analyses were performed using GraphPad Prism 5. All data sets were tested for normal distribution using a Kolmogorov-Smirnov test (with Dallal-Wilkinson-Lilie for P value) and a D'Agostino and Pearson omnibus normality test. Two-tailed Student's t test for (un)paired data was applied as appropriate. In the absence of normal distribution, significance was determined by a Mann-Whitney test or a Wilcoxon's matched-pairs signed-rank test for paired data. Uniform or random distribution was assessed using the Rayleigh uniformity test using ImageJ software (NIH).

RESULTS

EFs stimulate human macrophages to migrate directionally

We first determined if human monocyte-derived macrophages respond to EFs by analyzing whether their migration was altered

by an externally applied EF, similar in strength to those found physiologically at skin wounds (150 mV/mm) [8–10]. Time-lapse video microscopy was used to track cell movement over 2 h (Fig. 1A and B). Without EF stimulation, human macrophages migrated randomly in all directions (Fig. 1C and E and Supplemental Video 1). In contrast, macrophages exposed to the EF showed consistently strong directional migration, with $84.9 \pm 3.4\%$ of cells migrating toward the anode (Fig. 1D and F and Supplemental Video 1). The directedness of migration (negative value indicates anodal migration; see Materials and Methods and Supplemental Fig. 1B) was skewed significantly by EF exposure compared with cells without an EF (0.04 ± 0.05 vs. -0.56 ± 0.08 ; $z < 0.01$; Fig. 2A). The Tt/T of EF-exposed macrophages was comparable to controls migrating without an EF (50.5 ± 6.4 μ m/h vs. 46.2 ± 4.4 μ m/h; Fig. 2B). However, final Td/T following EF stimulation was increased significantly (19.3 ± 2.9 μ m/h vs. 25.2 ± 3.2 μ m/h; $P < 0.01$; Fig. 2C). Therefore, EFs of 150 mV/mm induced significant anodal migration by macrophages, without increasing the speed or overall distance of migration.

Anode-directed cell migration was voltage dependent between 50 and 300 mV/mm (Fig. 2D) and still evident at field strengths as low as 5 mV/mm (Supplemental Fig. 2). At 50 mV/mm, $69 \pm 0.4\%$ of macrophages migrated to the anode, compared with $93 \pm 5\%$ at 300–450 mV/mm (Fig. 2E). By contrast, migration of non-EF-exposed control cells did not show a directional preference, with equivalent proportions of macrophages migrating randomly (Rayleigh uniformity test, $P = 0.378$). In keeping with data obtained at 150 mV/mm, EF strength affected the final Td but not the Tt/T (Fig. 2F), with a peak Td/T of 39.6 ± 7.8 μ m/h at 300 mV/mm (Fig. 2G).

The question arises as to whether the effects of EFs on macrophage migration are replicated by the progenitor monocyte population. Monocytes exposed to EFs of 150 mV/mm also showed strong directional migration but to the cathode rather than the anode (Fig. 3A and E), with $73.6 \pm 5.4\%$ of monocytes migrating directionally to the cathode; by contrast, non-EF-exposed controls migrated randomly (Fig. 3A and D). This difference in directional movement between monocyte and macrophages was retained, irrespective of macrophage activation state, with $68.3 \pm 3.1\%$ of M1 macrophages and $67.5 \pm 3.0\%$ of M2 macrophages versus $70.1 \pm 4.5\%$ of nonactivated control macrophages showing anodal migration. Moreover, unlike macrophages, EF stimulation enhanced the Tt/T (Fig. 3B) and the Td/T (Fig. 3C) of monocytes (164.9 ± 29.4 vs. 171.8 ± 6.9 μ m/h and 37.3 ± 9.0 vs. 290.9 ± 9.8 μ m/h, respectively). Thus, the character of the macrophage electrotactic response to EFs is highly specific to the more mature cell type.

EF stimulation reorganizes the macrophage actin cytoskeleton

Microscopic examination revealed that EF exposure results in a spatial and structural reorganization of macrophages, in addition to directed migration. After 2 h of EF exposure, macrophages adopted a strikingly extended and polarized shape with a leading edge facing anodally (Fig. 1B). Although total cell area was not changed by EFs (Fig. 4A), many macrophages became significantly more elongated (Fig. 4B) and aligned horizontally and

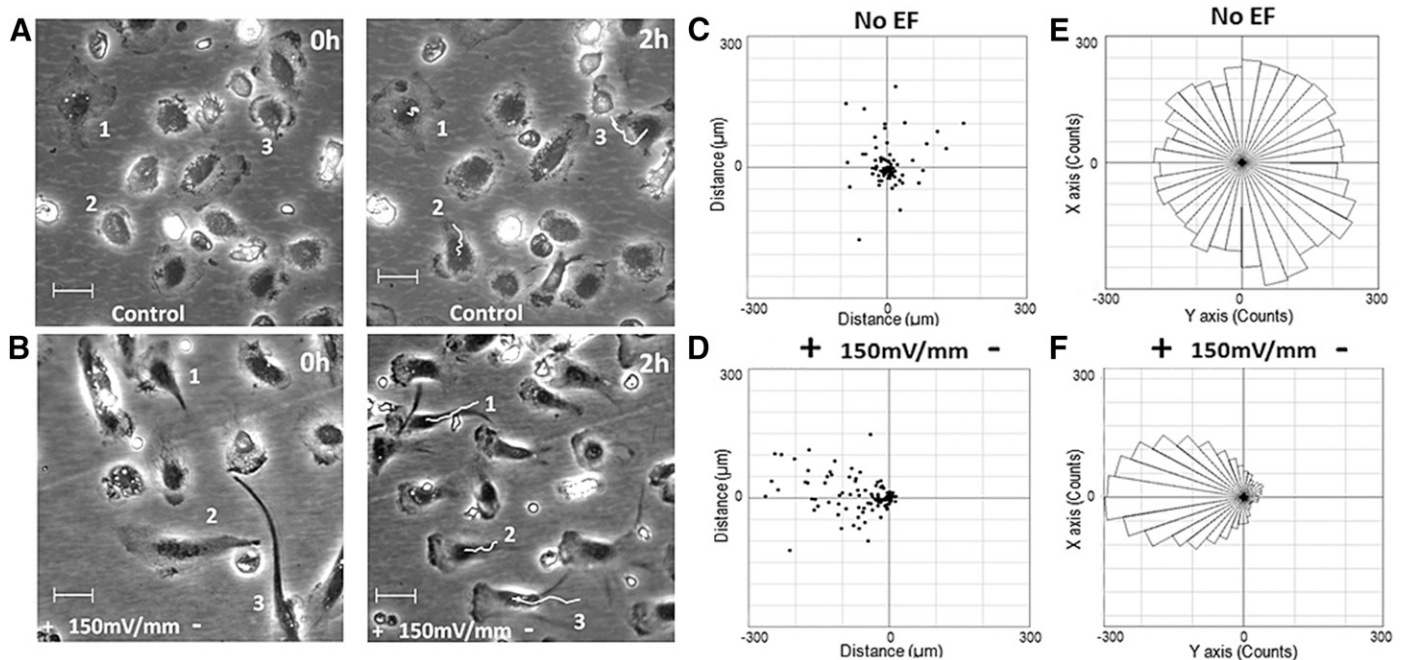


Figure 1. Human macrophages migrate directionally to the anode. Time-lapse images of human macrophage migrating with (A) no stimulation and (B) EF of 150 mV/mm. Numbers in white (1, 2, 3) indicate start and end positions of cells over a 2 h period. Cell paths were tracked using ImageJ software (NIH). Images are representative of independent experiments from 8 individual donor macrophage preparations. Original scale bars, 60 μ m. (C and D) Migrational Td of cells over a 2 h period. Each point represents the final position of a single cell relative to their starting position at 0 h at the origin. (E and F) Distribution of migration angles were calculated from x - y coordinates at the beginning and end of the 2 h cell track (see Supplemental Fig. 1). Angles are grouped in 10° intervals, with the radius of each wedge indicating numbers of cells. Rayleigh uniformity test was used to confirm if distribution was uniform. (C–F) All data are representative of independent experiments from 8 individual macrophage preparations; ≥ 100 cells analyzed for each donor.

parallel to the field vector (Fig. 4C). These cells, referred to from this point as “polarized in response to EFs,” constitute $42 \pm 4\%$ of the total macrophage population. In all experiments, control macrophages not exposed to EFs displayed random orientations, as assessed by the Rayleigh uniformity test.

The distribution of polymerized actin in EF-treated macrophages was examined, as coordinated actin dynamics control cell shape and movement, whereas the polarized distribution of podosomes, major actin-rich adhesion structures in macrophages, regulates migration. Untreated, control macrophages displayed a rounded shape and randomly distributed podosomes with a uniform, peripheral distribution of actin (Fig. 4D, left). In contrast, polymerized actin and podosomes were polarized toward the leading, anode-facing edge of EF-responsive macrophages (Fig. 4D, right). Thus, EFs induced significant changes ($P < 0.0001$) in actin distribution in polarized cells (Fig. 4E), conducive to the observed directional macrophage migration.

EF stimulation up-regulates phagocytic activity

A key functional property of macrophages is the uptake and clearance of microbes, apoptotic cells, and cellular debris [18]; therefore, we investigated the effects of EF exposure on phagocytic activity. Macrophages that had been exposed to 150 mV/mm for 2 h and then removed from the EF demonstrated significantly increased phagocytosis of carboxylate microspheres (Fig. 5A, left) compared with uptake by untreated control cells. The macrophage microsphere phagocytic uptake

rose from $26.6 \pm 3.3\%$ to $37.5 \pm 4.3\%$ ($P = 0.014$; $n = 6$), an increase over baseline phagocytosis of 42.2% (Fig. 5B). Strikingly, macrophage preparations from every human donor tested ($n = 6$) displayed such increased phagocytic responses. Furthermore, EFs of 150 mV/mm enhanced significantly the PI of macrophages, from 43.7 ± 9.8 to $66.9 \pm 12.0\%$ ($P < 0.05$; 53% over baseline), again reflecting the greater overall efficiency of clearance by EF-exposed macrophages. Increases in the percentage phagocytic uptake and PI were also observed when macrophages were exposed to EFs of even lower field strengths, and the magnitude of uptake was voltage dependent. The percentage phagocytosis rose from $16.7 \pm 2.4\%$ to $20.3 \pm 0.5\%$ at 50 mV/mm and to $23.7 \pm 2.3\%$ at 100 mV/mm, increases over background phagocytosis of 25% and 48%, respectively, whereas PI increased from 28.4 ± 5.0 to 35.0 ± 3.8 at 50 mV/mm and to 46.0 ± 7.2 at 100 mV/mm. These EF-induced effects would be predicted to stimulate biologically relevant increases in macrophage phagocytosis in physiologic settings.

The next question was whether EFs also induced phagocytic activity for particles of pathologic relevance and of targets that are recognized by different receptors. We analyzed the uptake of the nominal opportunist pathogen *C. albicans* and of apoptotic neutrophils, representative of cells that need to be cleared for wound resolution (Fig. 5A, middle and right, respectively). As with the carboxylate microspheres, EF exposure resulted in a significant increase ($P = 0.035$) in the percentage phagocytosis of *C. albicans* ($48.2 \pm 5.4\%$; $n = 5$) compared with unstimulated

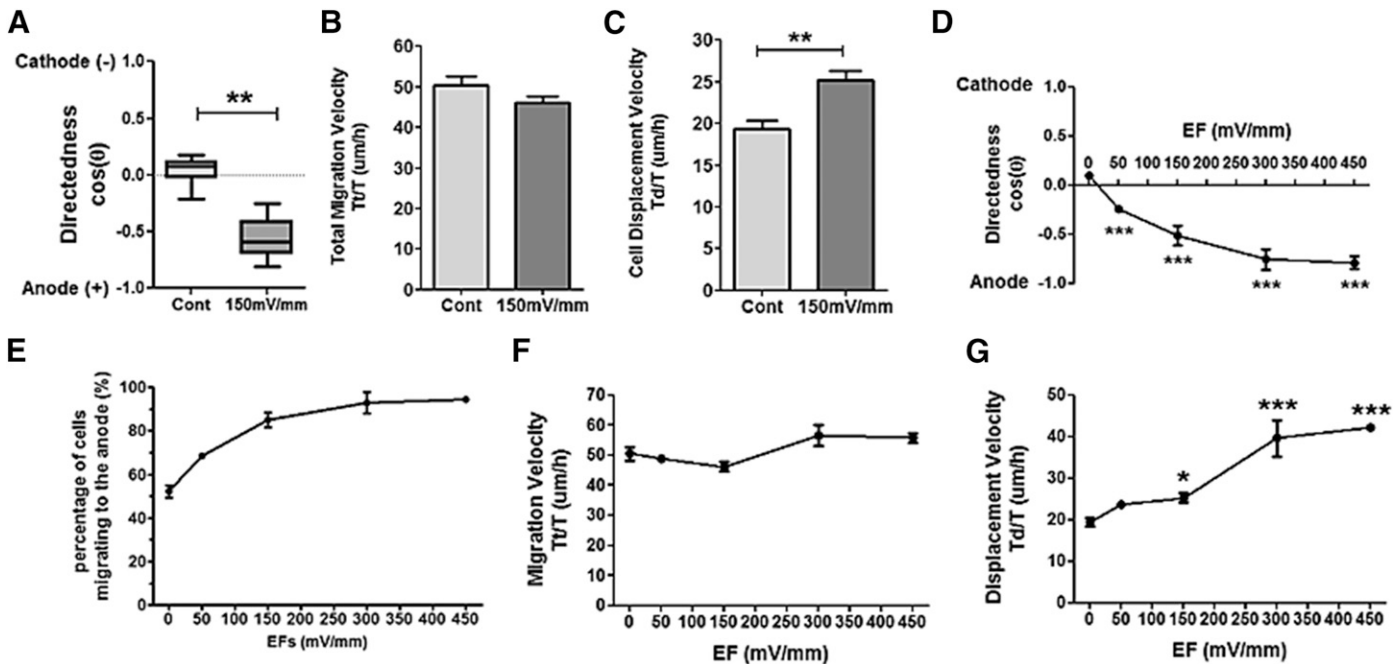


Figure 2. Anode-directed cell migration is voltage dependent. Migration of human macrophages in 150 mV/mm EFs. (A) Directedness of cell migration [cos(θ)], (B) Tt/T, (C) Td/T. Data shown as means \pm SEM of independent experiments from 8 individual macrophage preparations; ≥ 100 cells analyzed for each donor. Cont, Control. (D–G) Migration of human macrophages in response to EFs of increasing strength. (D) Directedness of migration. (E) Percentage of cells migrating to the anode. (F) Tt/T. (G) Td/T. Data shown as means \pm SEM of independent experiments from 8 individual macrophage preparations. One-way ANOVA; * $P < 0.05$, ** $P < 0.01$, *** $P < 0.001$.

cultures ($39.8 \pm 2.8\%$, $n = 5$; Fig. 5C), and uptake of apoptotic neutrophils was also enhanced ($8.7 \pm 1.7\%$ vs. $11.2 \pm 1.7\%$; $P = 0.001$; $n = 5$; Fig. 5D). Likewise, EFs increased the PI for *C. albicans* and apoptotic neutrophils from $102.1 \pm 9.8\%$ to $119.4 \pm 17.2\%$ and from $11.0 \pm 2.3\%$ to $14.9 \pm 3.2\%$, respectively. As with the carboxylate beads, the clearance efficiency over baseline of *C. albicans* and apoptotic neutrophils was greater following EF exposure, by 16.9% and 35.5%, respectively. Taken together, these results indicate that EFs enhance phagocytic activity significantly in response to diverse challenges, including those relevant to wound clearance.

EFs polarize phagocytic receptors

One explanation for the EF-enhanced phagocytic uptake by macrophages would be that the relevant receptors become more effective, because they cluster. To test this, we examined changes in the distributions of representative phagocytic receptor types in response to EFs. The mannose receptor (Fig. 6A) mediates uptake of *C. albicans*, whereas the scavenger receptor 1 (Fig. 6B) contributes to the uptake of carboxylate beads and apoptotic cells. Analyses of the 2 stained receptors revealed that whereas they were distributed evenly over the surface of individual unstimulated macrophages, both became polarized to occupy the anode facing half of the cells after exposure to EFs (Fig. 6C and D). In neither case was total fluorescence across the whole cell changed, indicating that the receptors were redistributed but not up-regulated. It was also tested using live tracking, over 1 h, whether the level of phagocytic activity was related to the shape change of macrophages that occurred under EF exposure. It was

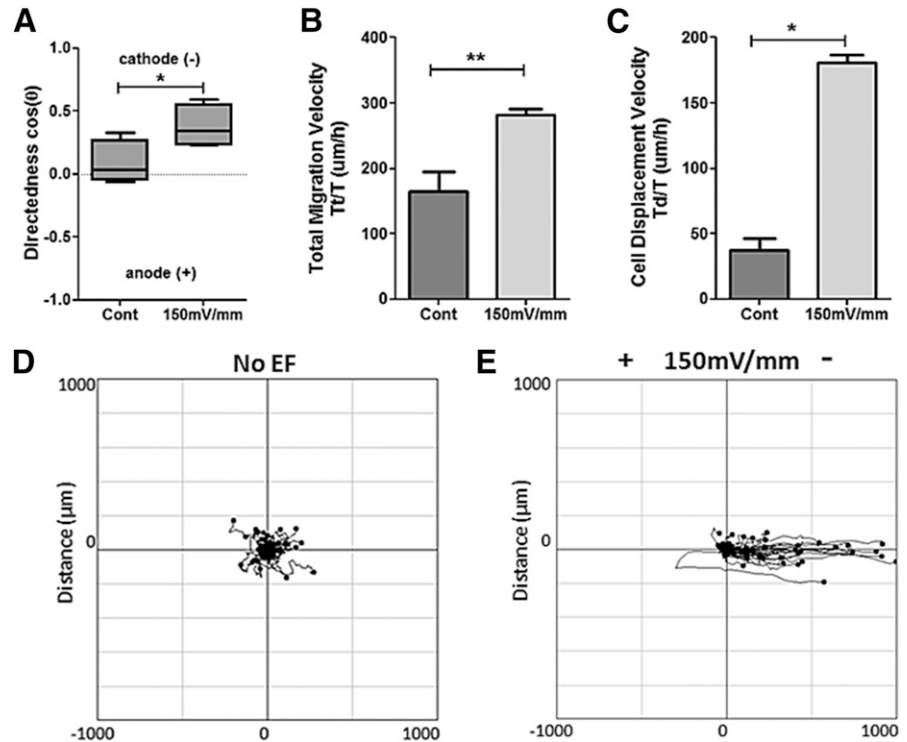
observed that EF-polarized cells were responsible for 62.3% of all the phagocytic events (27.4% of the elongated cells were actively phagocytic vs. 16.7% of cells that were not elongated; Fig. 6E). Critically, the EF shape-polarized macrophages preferentially engaged with and engulfed particles at the anode-facing section of their membrane, where receptor clustering was prominent (Fig. 6F). In contrast, neither control-unstimulated macrophages nor those that failed to change shape under EF showed any preference for the location of phagocytic uptake on the cell surface. These results support a model, whereby the EF-induced redistribution and clustering of receptors in macrophages contribute to the overall increase in phagocytosis.

EFs activate PI3K and p-ERK and mobilize intracellular Ca^{2+}

We next tested potential intracellular mechanisms by which EFs direct migration and phagocytic activity. The PI3K, p38, ERK1/2, and STAT3 signaling pathways were examined, as these have been reported to be activated by physical stimuli and to drive actin-induced cytoskeletal changes in other cell types [16, 19]. The levels of p-Akt, used as a marker of PI3K activity, were increased in macrophages exposed to EFs (Fig. 7A and B), in line with a role in the EF signaling cascade. ERK activity was also induced by EFs (Fig. 7A and C), whereas there was no activation of STAT3 nor any significant changes in p38 activity, showing that the EF-induced effects were specific.

EF-mediated effects on intracellular Ca^{2+} were measured, as these mediate many macrophage responses [20, 21]. Exposure to EFs caused a gradual rise in intracellular Ca^{2+} above steady

Figure 3. Human monocytes migrate directionally to the cathode in response to EFs (150 mV/mm). (A) Directedness of cell migration, (B) Tt/T, (C) Td/T. Data shown as means \pm SEM. (D and E) Migrational Td of a population of cells over a 2 h period. Each point represents the final position of a single cell relative to their starting position at 0 h at the origin. Data are representative of 3–4 independent experiments; >100 cells were analyzed for each donor. Paired *t* test; **P* < 0.05, ***P* < 0.01.



background levels, peaking 2.4 min after stimulation (Fig. 7D). This was seen in $53.8 \pm 11.4\%$ of the macrophages. Collectively, the results suggest a mechanism, whereby EFs initiate intracellular signaling pathways in macrophages that trigger actin polymerization, leading to enhancement of immune functions, including migration and phagocytosis.

PI3K is critical to drive downstream pathways essential for all types of phagocytosis. To determine the relevance of the up-regulated PI3K activity in driving EF-enhanced macrophage phagocytosis, we examined the effect of preincubation with the well-known PI3K inhibitor, LY294002 [15]. As shown previously, EF exposure resulted in an increase in bead uptake ($42.6 \pm 5.4\%$ increase) and the PI ($72.5 \pm 11.3\%$ increase; Fig. 7E and F). LY294002 preincubation inhibited baseline phagocytosis by $25.2 \pm 2.0\%$ in non-EF-exposed control macrophages, in line with the importance of this pathway for bead uptake. PI3K inhibition also attenuated the enhanced uptake observed in EF-exposed macrophages by 44.8% (Fig. 7E) and the increase in the PI by 41.3% (Fig. 7F), confirming that PI3K is an essential component of the EF-enhanced phagocytosis. However, the EF-induced effects were not abrogated fully, implying that the up-regulated PI3K activation is not the sole mediator through which EFs signal.

Inhibition of PI3K on EF-induced anodal distribution of polymerized actin and scavenger receptor clustering was also determined to confirm the relevance of this pathway on the macrophage responses. As Erk activity and Ca^{2+} mobilization were increased by EF application (Fig. 7C and D), and LY294002 alone did not completely inhibit phagocytosis, EF-induced responses were compared after their inhibition by U0126 (ERK1/2 inhibitor), BAPTA-AM (specific intracellular Ca^{2+} chelator), and BAPTA (extracellular Ca^{2+} chelator). As with phagocytosis, following PI3K inhibition, the EF-induced anodal

distribution of polymerized actin was decreased significantly, with a $44.3\% \pm 0.6$ reduction (Fig. 7G). A decrease ($63.1\% \pm 2.2$) in EF-induced clustering of the scavenger receptor was also observed following PI3K inhibition (Fig. 7H). Inhibition of ERK1/2 activity, depletion of intracellular Ca^{2+} , or chelation of extracellular Ca^{2+} also attenuated EF-induced actin polarization ($35.4\% \pm 0.4$, $39.8\% \pm 12.3$, and $54.1\% \pm 17.7$; respective mean values \pm sd; $n = 3$) and scavenger receptor A clustering ($48.4\% \pm 3.0$, $44.2\% \pm 1.5$, and $67.3\% \pm 11.5$; respective mean values \pm sd; $n = 3$), although changes did not reach statistical significance (Fig. 7G and H). Overall, the results show that EF-induced PI3K, ERK, and Ca^{2+} signaling are each important for the magnitude of EF-induced changes in macrophage-directed migration and phagocytosis. However, none of the inhibitors completely abrogated EF-induced responses, indicating that integration of multiple signaling pathways is required to fully drive EF-mediated effects.

EFs modulate macrophage cytokine secretion

Macrophages activated by chemical mediators, such as IFN- γ , LPS, or IL-4, adopt strong, functional phenotypes that produce different cytokine-release patterns. Therefore, we asked whether the responses of macrophages to EFs also included effects on cytokine secretion. EF exposure moderately increased the production of TNF- α (Fig. 8A), with no significant change in CCL2 or IL-10 levels (Supplemental Table 1). NT3, a well-defined healing mediator, associated with M2 macrophages [22, 23], also was increased significantly (Fig. 8A), whereas the secretion of the proresolving mediators VEGF and TGF- β 1 was unchanged by EF stimulation. Given that macrophages also are subject to soluble inflammatory mediators in damaged tissue, we examined the combined effects of M1 polarization using IFN- γ and LPS, together with EF exposure. As expected, IFN- γ /LPS

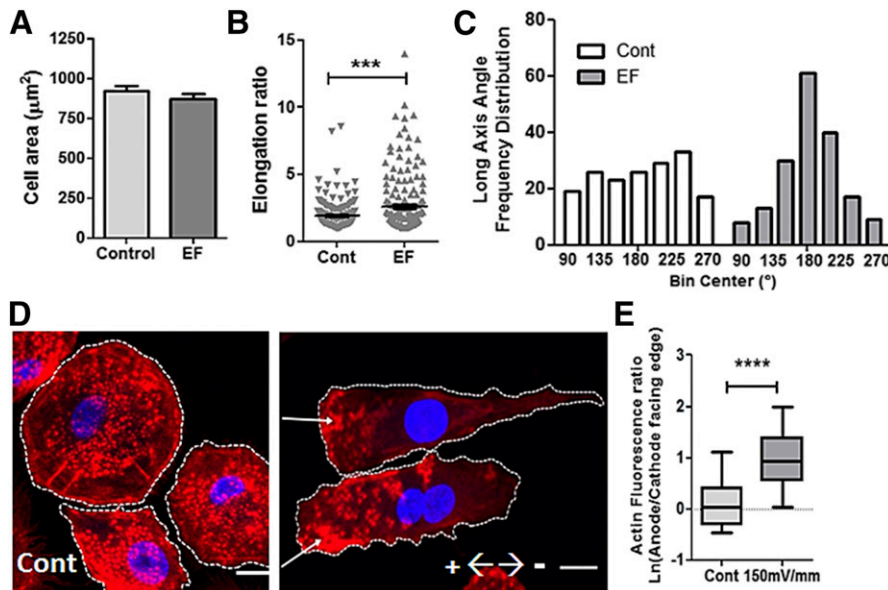


Figure 4. EFs induce cytoskeletal rearrangement in human macrophages. (A) Cell area (μm^2). (B) Cell elongation ratio (long axis:short axis). Unpaired *t* test; *****P* < 0.001. (C) Distribution of the long axis angle ($^\circ$). The measurements are illustrated schematically (see Materials and Methods and Supplemental Fig. 1). (D) Confocal microscopy images of human macrophages following no stimulation and stimulation with EF (150 mV/mm) for 2 h. Two cells aligned parallel to the EF vector are shown. Images were taken at $\times 40$ magnification using a confocal fluorescence microscope. Cells stained with phalloidin (F-actin, red) and Vectashield with DAPI (nuclear stain, blue). Original scale bars, 10 μm . (E) Actin fluorescence ratio between the left (anode facing) and right (cathode facing) edge of cells. Images and data (shown as means \pm SEM) are representative of independent experiments from 4 individual macrophage preparations (in duplicate); ≥ 30 cells measured for each condition. Ln, natural log. Unpaired *t* test; *****P* < 0.0001.

activation induced a significant increase in the proinflammatory cytokines IL-1 β , IL-6, IL-23, TNF- α , and IL-10 and nitrite levels. EF costimulation, in addition to IFN- γ /LPS, resulted in selective and additive increases in IL-1 β and IL-23 secretion (Fig. 8B) but did not further enhance the IL-6, TNF- α , IL-10, and nitrite responses. By contrast with the augmentation of particular M1 responses, the effects of EF costimulation on IL-4-activated macrophages were weaker, with a trend toward enhanced TNF- α secretion and no changes to the production of VEGF, IL-10, or TGF- β (Supplemental Table 1). Although the responses were subtle, overall, exposure of human macrophages to EFs alone or in combination with conventional stimuli does modulate the secretion of cytokines relevant to inflammation and healing.

DISCUSSION

We show for the first time that EFs of physiologic strength direct human macrophage migration and are a key determinant of multiple macrophage functions, including phagocytosis and cytokine secretion. Many of these responses may be attributed to polarization of surface phagocytic receptors, EF-induced mobilization of intracellular Ca^{2+} , activation of the intracellular signaling mediators, PI3K and ERK, and reorganization of the actin cytoskeleton. Overall, EFs emerge as an important, but previously overlooked, physical cue that regulates macrophage properties highly relevant to resolution of injury or infection.

Conventional models hold that immune cells are recruited toward infected or injured tissue by diffusible molecular gradients of "damage signals," such as chemokines [18, 24]. Our data reveal that human macrophages also exhibit electrotactic migration in response to EFs, adding EFs to the list of key damage signals and introducing a radical new concept in our understanding of how immune cells are positioned and activated during infection and tissue repair. Electrotaxis of macrophages is at least as directionally efficient as chemotaxis in response to

growth factors [25, 26], and macrophages respond to both classes of stimuli by rapidly adopting a similar, polarized morphology with a distinctive leading lamellipodium and a smaller, pointed trailing edge [27–29]. This elongated shape is aligned parallel to the EF vector, which makes movement efficient and would facilitate macrophage migration through tissue. Macrophage elongation has been shown to polarize murine macrophages to a M2 phenotype [4], and M2 polarization is associated with enhanced migration [30]. However, our data argue against macrophage elongation as the major mechanism by which externally applied EFs influence human macrophage functions in our study, as the 2 types of stimuli exert different effects. Thus, EF-exposed macrophages did not show the significant up-regulation in M2 activation markers nor the decrease in secretion of proinflammatory markers that was associated previously with shape-polarized macrophages [3, 4].

It is striking that electrotaxis of human macrophages was directed to the anode, in contrast to the cathodal migration seen here for monocytes and reported for lymphocytes [31]. Anodal migration of rodent macrophages has also been described [32], albeit under a direct, current EF, 2.5- to 8-fold greater than the maximum EF we used, supporting our view that the directional response exhibited by macrophages is unique among immune cell types tested to date. The opposing migrational directionality by cells of similar origin is not exclusive to monocytes/macrophages. For example, bovine epithelial cells from the apex and the equator of the eye lens migrate in opposite directions [33], and fish keratocytes migrate to the cathode, whereas keratocyte cell fragments migrate to the anode [34]. Physiologic EFs also have diverse, unexplained effects on migration of fibroblasts from different origins, with bovine ligament fibroblasts migrating to the cathode, corneal stroma and pulmonary artery fibroblasts migrating anodally, and human skin fibroblasts failing to migrate directionally [35–39]. In common with these examples, the precise identity of factors that govern oppositely directed migration of human macrophages and their monocyte

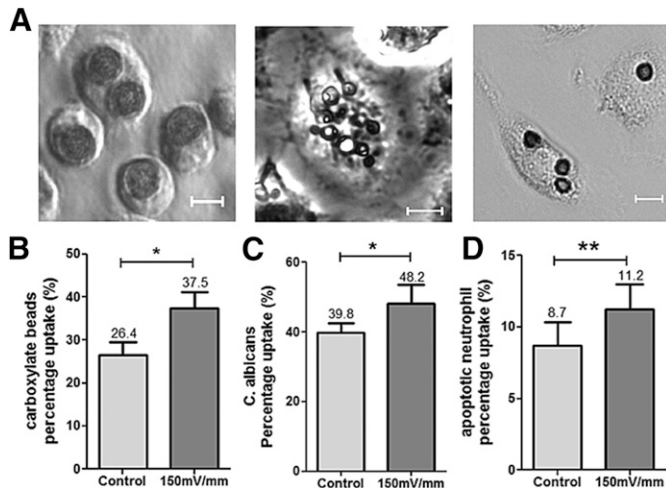


Figure 5. EFs increase human macrophage phagocytic uptake. Macrophages were exposed to an EF (150 mV/mm) for 2 h and then cultured with specific particles for a further 2 h. (A) Endpoint images following bead uptake (left), *C. albicans* (middle), and apoptotic neutrophils (right). Images shown are representative of independent experiments. Original scale bars, 10 μ m. Percentage uptake of (B) carboxylate beads, (C) *C. albicans*, and (D) apoptotic neutrophils. Data shown as means \pm SEM of independent experiments from at least 5 individual macrophage preparations. Paired *t* test; **P* < 0.05, ***P* < 0.01.

precursors in low-strength EFs are challenging and unresolved questions. The reversal may reflect inherent differences in the composition of charged molecules, such as glycosylated proteins (including integrins and receptors), in the plasma membrane, which change as monocytes mature [40]. Another possibility is differences for monocytes and macrophages in key signaling pathways integrating EFs, such as phosphatidylinositol (3,4,5)-trisphosphate/phosphatase and tensin homolog or other activator/inhibitor ratios, which control the direction of cell migration [34]. Competing pathways can bias signaling spatially at the front and rear of the cell to orient it and guide migration. These divergences of responsiveness to endogenous EFs raise questions as to whether differential activation of macrophages could influence their migration patterns. However, neither M1 nor M2 activation altered macrophage anodal migration, highlighting the consistency of strong directed migration in this mature cell type.

The "reversed" direction of EF-induced electrotaxis of monocytes following maturation to macrophages may be related to their functions in repair. EFs generated, for example, in wounds would play an important role in attracting monocytes from blood vessels, but after they infiltrate into tissue and mature into macrophages, EFs may subsequently contribute to the positioning and priming of these cells to restore tissue homeostasis through phagocytosis, cytokine secretion, and angiogenesis. In this context, it may be particularly relevant that dermal areas of wounded skin exhibit a predominance of mature macrophages, and this area is thought to be more positively charged than the wound center [41], consistent with our observation of anodal macrophage migration.

A key and provocative result is that EFs significantly enhanced phagocytic uptake of carboxylate beads, yeast, and apoptotic

neutrophils, which engage different classes of cell surface receptors on human macrophages [42]. Two mechanisms common to each of these targets may explain such a general increase in the phagocytosis efficiency. First, EFs polarized mannose and scavenger receptors to the anode-facing side of macrophages without increasing their expression, and such skewed redistribution leads to localized receptor clustering that may lower the threshold to trigger phagocytosis. Secondly, as with cell migration, phagocytosis is an actin-driven process, and following receptor binding, the EF-induced polarization and accumulation of actin at leading edges of macrophages would facilitate the formation of membrane ruffles and the extension of pseudopodia to enhance internalization. This EF-induced uptake has important implications for resolution of injury, as efficient phagocytic clearance of apoptotic cells is critical for restoring

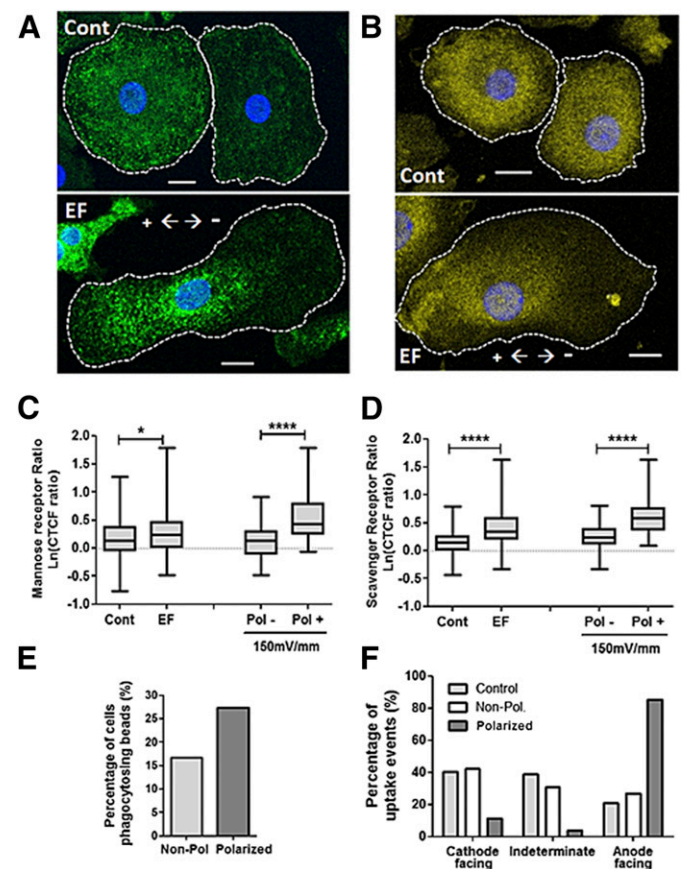


Figure 6. EF-induced uptake is associated with the polarization of phagocytic receptors. Representative images of (A) mannose receptor and (B) scavenger receptor distribution on human macrophages. Confocal images $\times 40$; original scale bars, 10 μ m. Receptor fluorescence ratio in human macrophages of the mannose receptor (C) and scavenger receptor (D). The ratio was described as the total cell fluorescence of the left hemisphere to that of the right hemisphere. Ratios were compared between control and EF-exposed cells and within EF-exposed macrophage populations, between cells that polarized (Pol+) and cells that did not polarize (Pol-; Non-Pol). Data shown are representative of 3 individual experiments. Mann-Whitney test; **P* < 0.05, *****P* < 0.0001. (E) Percentage of phagocytic human macrophages, according to polarization state under EF. (F) Distribution of uptake events, according to location around cell membrane.

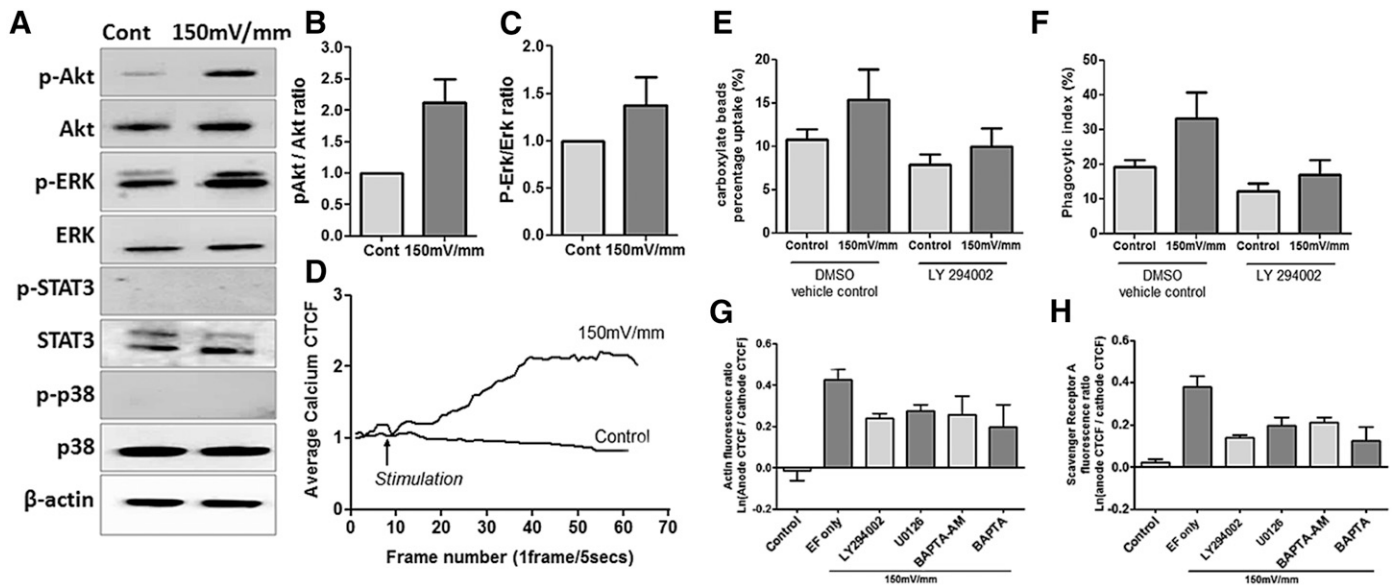


Figure 7. EF stimulation activates PI3K/Akt, and Erk pathways mobilize intracellular Ca^{2+} in human macrophages. (A) Representative Western blots of p-Akt/Akt, p-Erk/Erk, p-STAT3/STAT3, p-p38/p38, and β -actin. Macrophages were stimulated with 150 mV/mm EFs for 2 h. Ratio of p-Akt/Akt (B) and p-Erk to Erk (C) band intensity, as determined by densitometry. Shown as means \pm SEM (normalized to controls) of independent experiments from 4 individual macrophage preparations. Average Fluo-4 AM fluorescence traces (D) showing the change of fluorescence (representing Ca^{2+} mobilization) over time following application of no stimulation and 150 mV/mm in responding human macrophages. Data represent mean of independent experiments from at least 3 individual macrophage preparations. Macrophages were treated with 10 μM InSolution LY294002 or DMSO for 1 h, exposed to 150 mV/mm for 2 h, and incubated with 10 μM carboxylate beads for 2 h. (E) Percentage uptake of carboxylate beads, shown as means \pm SEM of independent experiments from 3 individual macrophage preparations. (F) PI, calculated as the mean number of particles engulfed per phagocytosing macrophages, multiplied by the percentage of phagocytic cells. Data represent mean of independent experiments from 3 or more individual macrophage preparations. Macrophages were left untreated or treated with LY294002 (10 μM), U0126 (10 μM), BAPTA-AM (10 μM), or BAPTA (300 μM) for 30 minutes before EF exposure and determination of Actin distribution as shown by the Actin fluorescence ratio between the left (anode facing) and right (cathode facing) edge of cells (G), or scavenger receptor A clustering as shown by receptor fluorescence ratio (total cell fluorescence of the left hemisphere to that of the right hemisphere) (H). Data (shown as mean \pm SEM) are representative of independent experiments from 3 individual macrophage preparations.

tissue homeostasis, not only by preventing excessive proinflammatory responses but also by switching on production of anti-inflammatory and wound-healing mediators, such as VEGF, TGF- β , and platelet-derived growth factor [13, 14, 43]. There is now compelling evidence that failure to remove apoptotic cells effectively promotes inflammation and impairs healing. EFs generated internally within wounded tissue would help drive macrophage phagocytosis and prevent these effects. Improved microbial clearance by macrophages also would contribute to the known anti-infective effects of wound-induced EFs [44]. The development of appropriate models of skin healing that allow manipulation of EFs in vivo will allow these predictions to be tested.

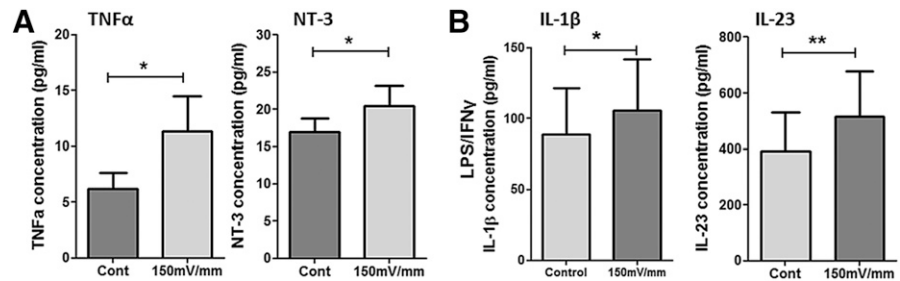
EFs elevated intracellular Ca^{2+} concentration and increased the activity of PI3K and ERK in macrophages, and the inhibition of their activity significantly attenuates the magnitude of EF-induced changes in actin polarization and receptor clustering. These intracellular mediators determine migratory directedness and motility during chemotaxis, suggesting that electrotaxis and chemotaxis share some common intracellular programs. Indeed, Ca^{2+} -induced activation of PI3K/p-AKT is reported to drive chemotactic migration in macrophages [45]. PI3K and ERK also mediate EF-induced effects in epithelial cells and neutrophils, and their genetic disruption drastically diminishes electrotaxis by these cell types [16]. Moreover, enhanced PI3K activity and Ca^{2+}

mobilization have well-established roles in driving phagocytosis by modulating the cytoskeleton and facilitating pseudopod extension, phagocytic cup closure, and phagosome maturation [46]. This is in keeping with our proposed model that EFs activate intracellular signaling, driving downstream actin changes to enhance phagocytic activity.

Exposure of human macrophages to EFs enhanced secretion of particular cytokines, but this was modest. The levels of TNF- α induced with EF exposure or simultaneous IL-4 and EF exposure, for example, did not reach levels induced by M1 activation. However, these changes may be of biologic relevance, as they were similar in magnitude to those secreted by isolated wound macrophages that stimulate neighboring cells to engage in repair [47, 48]. Overall, EF exposure can modulate aspects of macrophage polarization, but the more striking effects are to induce directional migration and enhance phagocytosis significantly.

In addition to introducing a new concept in understanding the natural processes of inflammation and wound repair, our findings are highly relevant to emerging clinical therapies that use EF stimulation. EF-based devices are effective clinically in the treatment of nonhealing wounds in patients with, for example, pressure ulcers or diabetes [49, 50], but the mechanisms responsible are poorly understood [51]. Until recently, the beneficial effects have been attributed to stimulation of epithelial

Figure 8. EF stimulation selectively enhances macrophage cytokine secretion. Macrophages were stimulated with 150 mV/mm EFs for 2 h without (A) or with (B) 100 ng/ml LPS and 20 ng/ml IFN- γ . Concentrations of TNF- α , NT3, IL-1 β , and IL-23 were measured, 24 h after stimulation. Data shown are representative of independent experiments from at least 7 individual macrophage preparations. Wilcoxon's matched-pairs signed-rank test; * $P < 0.05$, ** $P < 0.01$.



cell migration and division and to the anti-infective properties of the metallic, usually silver, electrodes, placed directly into the wound [52]. However, many nonhealing ulcers lack macrophages, with consequent poor clearance of apoptotic cells or production of prorepair mediators [13, 14]. Our data raise the possibility that EF devices may also correct this deficit by attracting, orienting, and enhancing the functions of macrophages within the wound site. These in vitro results raise important questions about naturally generated and clinically applied EFs and macrophage function, and in vivo effects will be the subject of our next studies.

Our discoveries contribute to a paradigm shift in the field of macrophage biology, with the increasing recognition that macrophages are responsive to physical cues. Following the recently described effects of substrate topography, cell shape, and elasticity [3–5] on macrophage function, we now report that human macrophages are regulated by EFs, which not only drive directed migration with a cell-specific anodal direction but also enhance cytokine production and phagocytic activity essential for clearance of infection and for tissue repair. These findings raise the prospect that EF-based therapies could be extended beyond tissue repair and ultimately, be exploited to modulate the function of macrophages in other inflammatory diseases where these cells are dysregulated.

AUTHORSHIP

J.I.H. was responsible for the study design; data acquisition, analysis, and interpretation; and critical revision of the draft. A.M.R. designed experiments and provided intellectual input, technical support, and materials. C.D.M. and R.N.B. designed experiments and provided intellectual input. H.M.W. designed experiments, provided supervision, analyzed data, and wrote the manuscript. All authors were involved in drafting the article or revising it critically for important intellectual content, and all authors read and approved the final manuscript.

ACKNOWLEDGMENTS

This work was supported by Kidney Research UK (Grant Number RP1/2012). J.I.H. was supported by an Institute of Medical Sciences University studentship. The authors thank the staff of the Aberdeen Microscopy and Histology Core Facility for advice and technical assistance. The authors also thank Christina E. Arnold for

guidance in initially setting up EFs and Jessica Becker, Jennifer Mitchell, and Robert Petrie for technical assistance in the laboratory. The authors acknowledge and are grateful to all volunteers for donating blood for macrophage and neutrophil isolation.

DISCLOSURES

The authors declare no conflicts of interest.

REFERENCES

- Murray, P. J., Wynn, T. A. (2011) Protective and pathogenic functions of macrophage subsets. *Nat. Rev. Immunol.* **11**, 723–737.
- Martinez, F. O., Sica, A., Mantovani, A., Locati, M. (2008) Macrophage activation and polarization. *Front. Biosci.* **13**, 453–461.
- McWhorter, F. Y., Davis, C. T., Liu, W. F. (2015) Physical and mechanical regulation of macrophage phenotype and function. *Cell. Mol. Life Sci.* **72**, 1303–1316.
- McWhorter, F. Y., Wang, T., Nguyen, P., Chung, T., Liu, W. F. (2013) Modulation of macrophage phenotype by cell shape. *Proc. Natl. Acad. Sci. USA* **110**, 17253–17258.
- Patel, N. R., Bole, M., Chen, C., Hardin, C. C., Kho, A. T., Mih, J., Deng, L., Butler, J., Tschumperlin, D., Fredberg, J. J., Krishnan, R., Koziel, H. (2012) Cell elasticity determines macrophage function. *PLoS One* **7**, e41024.
- Akan, Z., Aksu, B., Tulunay, A., Bilsel, S., Inhan-Garip, A. (2010) Extremely low-frequency electromagnetic fields affect the immune response of monocyte-derived macrophages to pathogens. *Bioelectromagnetics* **31**, 603–612.
- Zhou, S., Bachem, M. G., Seufferlein, T., Li, Y., Gross, H. J., Schmelz, A. (2008) Low intensity pulsed ultrasound accelerates macrophage phagocytosis by a pathway that requires actin polymerization, Rho, and Src/MAPKs activity. *Cell. Signal.* **20**, 695–704.
- Barker, A. T., Jaffe, L. F., Venable, J. W., Jr. (1982) The glabrous epidermis of cavies contains a powerful battery. *Am. J. Physiol.* **242**, R358–R366.
- Foulds, I. S., Barker, A. T. (1983) Human skin battery potentials and their possible role in wound healing. *Br. J. Dermatol.* **109**, 515–522.
- Nuccitelli, R., Nuccitelli, P., Li, C., Narsing, S., Pariser, D. M., Lui, K. (2011) The electric field near human skin wounds declines with age and provides a noninvasive indicator of wound healing. *Wound Repair Regen.* **19**, 645–655.
- Zhao, M. (2009) Electrical fields in wound healing—an overriding signal that directs cell migration. *Semin. Cell Dev. Biol.* **20**, 674–682.
- McCaig, C. D., Song, B., Rajnicek, A. M. (2009) Electrical dimensions in cell science. *J. Cell Sci.* **122**, 4267–4276.
- Lucas, T., Waisman, A., Ranjan, R., Roes, J., Krieg, T., Müller, W., Roers, A., Eming, S. A. (2010) Differential roles of macrophages in diverse phases of skin repair. *J. Immunol.* **184**, 3964–3977.
- Goren, I., Allmann, N., Yorgev, N., Schuermann, C., Waisman, A., Pfeilschifter, J., Frank, S. (2009) A transgenic mouse model of inducible macrophage depletion: effects of diphtheria toxin-driven lysozyme M-specific cell lineage ablation on wound inflammatory, angiogenic and contractive processes. *Am. J. Pathol.* **175**, 132–147.
- Arnold, C. E., Whyte, C. S., Gordon, P., Barker, R. N., Rees, A. J., Wilson, H. M. (2014) A critical role for suppressor of cytokine signalling 3 in promoting M1 macrophage activation and function in vitro and in vivo. *Immunology* **141**, 96–110.
- Zhao, M., Song, B., Pu, J., Wada, T., Reid, B., Tai, G., Wang, F., Guo, A., Walczyk, P., Gu, Y., Sasaki, T., Suzuki, A., Forrester, J. V., Bourne, H. R., Devreotes, P. N., McCaig, C. D., Penninger, J. M. (2006) Electrical signals control wound healing through phosphatidylinositol-3-OH kinase-gamma and PTEN. *Nature* **442**, 457–460.

17. Rajniecek, A. M., Foubister, L. E., McCaig, C. D. (2006) Temporally and spatially coordinated roles for Rho, Rac, Cdc42 and their effectors in growth cone guidance by a physiological electric field. *J. Cell Sci.* **119**, 1723–1735.
18. Koh, T. J., DiPietro, L. A. (2011) Inflammation and wound healing: the role of the macrophage. *Expert Rev. Mol. Med.* **13**, e23.
19. Stephens, L., Ellson, C., Hawkins, P. (2002) Roles of PI3Ks in leukocyte chemotaxis and phagocytosis. *Curr. Opin. Cell Biol.* **14**, 203–213.
20. Onuma, E. K., Hui, S. W. (1988) Electric field-directed cell shape changes, displacement, and cytoskeletal reorganization are calcium dependent. *J. Cell Biol.* **106**, 2067–2075.
21. Melendez, A. J., Tay, H. K. (2008) Phagocytosis: a repertoire of receptors and Ca(2+) as a key second messenger. *Biosci. Rep.* **28**, 287–298.
22. Shen, L., Zeng, W., Wu, Y. X., Hou, C. L., Chen, W., Yang, M. C., Li, L., Zhang, Y. F., Zhu, C. H. (2013) Neurotrophin-3 accelerates wound healing in diabetic mice by promoting a paracrine response in mesenchymal stem cells. *Cell Transplant.* **22**, 1011–1021.
23. Samah, B., Porcheray, F., Gras, G. (2008) Neurotrophins modulate monocyte chemotaxis without affecting macrophage function. *Clin. Exp. Immunol.* **151**, 476–486.
24. Cordeiro, J. V., Jacinto, A. (2013) The role of transcription-independent damage signals in the initiation of epithelial wound healing. *Nat. Rev. Mol. Cell Biol.* **14**, 249–262.
25. Chang, P. C. T., Sulik, G. I., Soong, H. K., Parkinson, W. C. (1996) Galvanotropic and galvanotactic responses of corneal endothelial cells. *J. Formos. Med. Assoc.* **95**, 623–627.
26. Webb, S. E., Pollard, J. W., Jones, G. E. (1996) Direct observation and quantification of macrophage chemoattraction to the growth factor CSF-1. *J. Cell Sci.* **109**, 793–803.
27. Hanley, P. J., Xu, Y., Kronlage, M., Grobe, K., Schön, P., Song, J., Sorokin, L., Schwab, A., Bähler, M. (2010) Motorized RhoGAP myosin IXb (Myo9b) controls cell shape and motility. *Proc. Natl. Acad. Sci. USA* **107**, 12145–12150.
28. Servant, G., Weiner, O. D., Herzmark, P., Balla, T., Sedat, J. W., Bourne, H. R. (2000) Polarization of chemoattractant receptor signaling during neutrophil chemotaxis. *Science* **287**, 1037–1040.
29. Veale, K. J., Offenhäuser, C., Lei, N., Stanley, A. C., Stow, J. L., Murray, R. Z. (2011) VAMP3 regulates podosome organisation in macrophages and together with Stx4/SNAP23 mediates adhesion, cell spreading and persistent migration. *Exp. Cell Res.* **317**, 1817–1829.
30. Vereyken, E. J. F., Heijnen, P. D. A. M., Baron, W., de Vries, E. H. E., Dijkstra, C. D., Teunissen, C. E. (2011) Classically and alternatively activated bone marrow derived macrophages differ in cytoskeletal functions and migration towards specific CNS cell types. *J. Neuroinflammation* **8**, 58.
31. Lin, F., Baldessari, F., Gyenge, C. C., Sato, T., Chambers, R. D., Santiago, J. G., Butcher, E. C. (2008) Lymphocyte electrotaxis in vitro and in vivo. *J. Immunol.* **181**, 2465–2471.
32. Orida, N., Feldman, J. D. (1982) Directional protrusive pseudopodial activity and motility in macrophages induced by extracellular electric fields. *Cell Motil.* **2**, 243–255.
33. Wang, E., Zhao, M., Forrester, J. V., McCaig, C. D. (2003) Bi-directional migration of lens epithelial cells in a physiological electrical field. *Exp. Eye Res.* **76**, 29–37.
34. Sun, Y., Do, H., Gao, J., Zhao, R., Zhao, M., Mogilner, A. (2013) Keratocyte fragments and cells utilize competing pathways to move in opposite directions in an electric field. *Curr. Biol.* **23**, 569–574.
35. Soong, H. K., Parkinson, W. C., Bafna, S., Sulik, G. L., Huang, S. C. M. (1990) Movements of cultured corneal epithelial cells and stromal fibroblasts in electric fields. *Invest. Ophthalmol. Vis. Sci.* **31**, 2278–2282.
36. Brown, M. J., Loew, L. M. (1994) Electric field-directed fibroblast locomotion involves cell surface molecular reorganization and is calcium independent. *J. Cell Biol.* **127**, 117–128.
37. Bai, H., McCaig, C. D., Forrester, J. V., Zhao, M. (2004) DC electric fields induce distinct preangiogenic responses in microvascular and macrovascular cells. *Arterioscler. Thromb. Vasc. Biol.* **24**, 1234–1239.
38. Finkelstein, E., Chang, W., Chao, P. H., Gruber, D., Minden, A., Hung, C. T., Bulinski, J. C. (2004) Roles of microtubules, cell polarity and adhesion in electric-field-mediated motility of 3T3 fibroblasts. *J. Cell Sci.* **117**, 1533–1545.
39. Chao, P. H., Lu, H. H., Hung, C. T., Nicoll, S. B., Bulinski, J. C. (2007) Effects of applied DC electric field on ligament fibroblast migration and wound healing. *Connect. Tissue Res.* **48**, 188–197.
40. McLaughlin, S., Poo, M. M. (1981) The role of electro-osmosis in the electric-field-induced movement of charged macromolecules on the surfaces of cells. *Biophys. J.* **34**, 85–93.
41. Mori, R., Kondo, T., Nishie, T., Ohshima, T., Asano, M. (2004) Impairment of skin wound healing in beta-1,4-galactosyltransferase-deficient mice with reduced leukocyte recruitment. *Am. J. Pathol.* **164**, 1303–1314.
42. Underhill, D. M., Goodridge, H. S. (2012) Information processing during phagocytosis. *Nat. Rev. Immunol.* **12**, 492–502.
43. Leibovich, S. J., Ross, R. (1975) The role of the macrophage in wound repair. A study with hydrocortisone and antimacrophage serum. *Am. J. Pathol.* **78**, 71–100.
44. Asadi, M. R., Torkaman, G. (2014) Bacterial inhibition by electrical stimulation. *Adv. Wound Care (New Rochelle)* **3**, 91–97.
45. Boudot, C., Saidak, Z., Boulanouar, A. K., Petit, L., Gouilleux, F., Massy, Z., Brazier, M., Mentaverri, R., Kamel, S. (2010) Implication of the calcium sensing receptor and the phosphoinositide 3-kinase/Akt pathway in the extracellular calcium-mediated migration of RAW 264.7 osteoclast precursor cells. *Bone* **46**, 1416–1423.
46. May, R. C., Machesky, L. M. (2001) Phagocytosis and the actin cytoskeleton. *J. Cell Sci.* **114**, 1061–1077.
47. Lee, S., Huen, S., Nishio, H., Nishio, S., Lee, H. K., Choi, B. S., Ruhrberg, C., Cantley, L. G. (2011) Distinct macrophage phenotypes contribute to kidney injury and repair. *J. Am. Soc. Nephrol.* **22**, 317–326.
48. Daley, J. M., Brancato, S. K., Thomay, A. A., Reichner, J. S., Albina, J. E. (2010) The phenotype of murine wound macrophages. *J. Leukoc. Biol.* **87**, 59–67.
49. Kloth, L. C. (2005) Electrical stimulation for wound healing: a review of evidence from in vitro studies, animal experiments, and clinical trials. *Int. J. Low. Extrem. Wounds* **4**, 23–44.
50. Centers for Medicare & Medicaid Services. (2002) *Medicare & Medicaid Statistical Supplement. 2002 Edition*. CMS.gov, Baltimore, MD.
51. Balakotounis, K. C., Angoules, A. G. (2008) Low-intensity electrical stimulation in wound healing: review of the efficacy of externally applied currents resembling the current of injury. *Eplasty* **8**, e28.
52. Polak, A., Franek, A., Taradaj, J. (2014) High-voltage pulsed current electrical stimulation in wound treatment. *Adv. Wound Care (New Rochelle)* **3**, 104–117.

KEY WORDS:

direct current · phagocytosis · migration · cytokines · wound repair